Zinc potentiates dopamine neurotransmission and cocaine seeking

Juan L. Gomez[1], Jordi Bonaventura[1], Jacqueline Keighron[2], Kelsey M. Wright[1], Dondre L. Marable[1], Lionel A. Rodriguez[1], Sherry Lam[1], Meghan L. Carlton[1], Randall J. Ellis[1], Chloe Jordan[3], Guo-hua Bi[3], Marco Pignatelli[4], Michael J. Bannon[5], Zheng-Xiong Xi[3], Gianluigi Tanda[2], Michael Michaelides[1, 6*]

[1]Biobehavioral Imaging and Molecular Neuropsychopharmacology Unit, National Institute on Drug Abuse Intramural Research Program, Baltimore, MD, 21224, USA

[2]Medication Development Program, National Institute on Drug Abuse Intramural Research Program, Baltimore, MD, 21224, USA

[3]Addiction Biology Unit, National Institute on Drug Abuse Intramural Research Program, Baltimore, MD, 21224, USA

[4]Department of Psychiatry and Taylor Family Institute for Innovative Psychiatric Research, Washington University School of Medicine, St Louis, MO 63110, USA

[5]Department of Pharmacology, Wayne State University School of Medicine, Detroit, MI, 48201, USA

[6]Department of Psychiatry, Johns Hopkins School of Medicine, Baltimore, MD, 21205, USA

*Correspondence:

Michael Michaelides, PhD

251 Bayview Blvd, Room 05A721A

Baltimore, MD 21224

Tel: +1-443-740-2894

Fax: +1-443-740-2734

mike.michaelides@nih.gov

Abstract

Cocaine binds to the dopamine transporter (DAT) in the striatum to regulate cocaine reward and seeking behavior. Zinc (Zn^{2+}) also binds to the DAT, but the *in vivo* relevance of this interaction is unknown. We found that cocaine abuse in humans correlated with low postmortem striatal Zn^{2+} content. In mice, cocaine decreased striatal vesicular Zn^{2+} and increased striatal synaptic Zn^{2+} concentrations and Zn^{2+} uptake. Striatal synaptic Zn^{2+} increased cocaine's *in vivo* potency at the DAT and was required for cocaine-induced DAT upregulation. Finally, genetic or dietary Zn^{2+} manipulations modulated cocaine locomotor sensitization, conditioned place preference, self-administration, and reinstatement. These findings reveal new insights into cocaine's pharmacological mechanism of action and indicate that Zn^{2+} can serve as a critical environmentally derived regulator of human cocaine addiction.

Introduction

Zinc (Zn^{2+}) is an essential trace element necessary for normal brain function (1-5). It is exclusively obtained via feeding and as the body lacks a specialized system for its storage, it needs to be obtained continuously to avoid a state of deficiency. Zn^{2+} is found in highest concentrations in the brain where it exists in two forms; a "fixed", protein-bound form, that serves as a catalytic co-factor or as a structural component to many proteins, and comprises ~90% of total brain concentration, and a "free", or labile form, comprising ~10% of total brain concentration. Zn^{2+} levels in the synaptic cleft are dependent on *Slc30a3*, a gene encoding a vesicular Zn^{2+} transporter (ZnT3) predominantly localized at neuron terminals that co-release glutamate (6, 7). Vesicular Zn^{2+} is released into the synapse upon neuronal activation, regulates neurotransmitter signaling, and plays important roles in brain disease (1-5), but its involvement in drug addiction is unknown.

Human drug abusers show dysregulated blood and hair Zn^{2+} content (8-13) but whether such deficits are involved in addiction to cocaine or other drugs is unclear. Cocaine binds to the dopamine transporter (DAT) to inhibit synaptic DA reuptake, which leads to an increase of extracellular DA (14). This mechanism underlies the direct subjective responses that accompany cocaine use (15), and is critical to cocaine self-administration in laboratory models, and cocaine reward and abuse liability in humans (16). Like cocaine, Zn^{2+} also binds to the DAT and promotes a conformation that inhibits DA uptake and, when cocaine is present, Zn^{2+} increases cocaine's affinity and modulates its potency to inhibit DA uptake in *in vitro* assays (17-21). Nevertheless, whether Zn^{2+} affects cocaine potency at DAT *in vivo* or whether it plays a role in cocaine's behavioral effects is unknown.

Methods

Subjects

De-identified postmortem human brain specimens were collected during the routine autopsy process as described in detail previously (46, 47). Briefly, the cause and manner of death were determined by forensic pathologists following medico-legal investigations that evaluated the circumstances of death including medical records, police reports, autopsy results, and toxicological data. Inclusion in the cocaine cohort (n = 20) was based on cocaine abuse as the cause of death, a documented history of drug abuse, and a toxicology positive for high levels of the cocaine metabolite benzoylecgonine and, in most cases, the short-lived cocaine adulterant levamisole, both

indicative of recent cocaine use prior to death. Control subjects (n=20) died as a result of cardiovascular disease or gunshot wound, had no documented history of drug abuse, and tested negative for cocaine and other drugs of abuse. Exclusion criteria for the study included a known history of neurological or psychiatric illness, death by suicide, estimated postmortem interval exceeding 20 hr, evidence of neuropathology (e.g. encephalitis, stroke), or chronic illness (e.g. cirrhosis, cancer, HIV, prolonged hospitalization). The final groups did not differ with regard sex, age, or race, nor with regard to brain pH, a well-established measure of sample quality and perimortem agonal state (48). Tissue from one cocaine user was not included due to very high cocaine metabolite levels.

Male C57Bl/6J mice were acquired from Jackson Labs at 8-weeks of age. Breeding pairs of *Slc30a3* (ZnT3) knockout mice were obtained from Dr. Thanos Tzounopoulos at the University of Pittsburgh and bred at the National Institute on Drug Abuse (NIDA) (Baltimore, MD) on a C57Bl/6J background. Mice were genotyped by Transnetyx (Cordova, TN) using tail snips. All mice were male and matched for age and weight. Mice were single-housed during experimental testing in a temperature and humidity-controlled environment on a regular light cycle (on at 7 am and off at 7 pm). Food and water were available ad libitum and mice were acclimated prior to any behavioral procedures by handling. All experimental procedures were carried out in accordance with the National Institutes of Health Guide for the Care and Use of Laboratory Animals and were approved by the Animal Care and Use Committee of NIDA.

Total Reflection X-ray Spectroscopy (TXRF)

Tissue samples were collected and weighed in 1.5 mL Eppendorf tubes. The weight of the tissue was directly used to calculate element concentrations in µg/kg units. Each tissue sample was dissolved in 100 µL of nitric acid (Sigma: NX0408) with 2 µL of a gallium standard (conc. 1000 ppm). Each sample was assessed in duplicate for TXRF elemental analysis using an S2 Picofox (Bruker, Billerica, MA). This instrument exposes the sample to an X-ray beam and measures fluorescence radiation specific to the element(s) of interest. Human samples were prepared from postmortem tissue collected from the anterior caudate. WT or ZnT3 KO mice received either saline, a single cocaine injection (20 mg/kg, i.p), or 8 repeated daily cocaine (20 mg/kg, i.p) injections and were euthanized 24 hrs after the last injection. 30 ppm and 5 ppm mice were exposed to each respective diet for 35 days and then euthanized. Mouse samples were prepared by slicing

flash frozen tissue on a cryostat (100 µm sections from Bregma 1.00 mm to 0.00 mm) and dissecting the cortex and striatum from each section.

Synchrotron X-ray Fluorescence Microspectroscopy (µXRFS)

Brain concentrations and distributions of Zn^{2+} from C57BL/6J mice injected with saline or cocaine (10 mg/kg, i.p.) every other day for 8 days and euthanized 24 hrs after the last injection were measured at the X26a beamline at the National Synchrotron Light Source (NSLS) at Brookhaven National Laboratory (Upton, NY). The synchrotron X-ray beam was tuned to 12 keV using a Si(111) channel-cut monochromotor. The monochromatic beam was then collimated to 350 µm×350 µm and then focused to approximately 6 µm×10 µm using Rh-coated silicon mirrors in a Kirkpatrick–Baez (KB) geometry. The sample was placed at a 45° angle to the incident X-ray beam and X-ray fluorescence was detected with an energy dispersive, 9-element germanium array detector (Canberra, Meriden, CT) oriented at 90° to the incident beam. The sample was approximately 6 cm from the detector. A light microscope objective (Mitutoyo, M Plan Apo 5X) was coupled to a digital CCD camera for sample viewing. Energy dispersive spectra were collected by raster-scanning the sample through the X-ray beam using a dwell time of 0.3 s/pixel and a step size of 10 µm. Zn Kα, fluorescence counts were then extracted from background-corrected energy dispersive spectra. All data were normalized to variations in incident photon flux by normalizing to changes in I0 measured by ion chamber upstream of the KB optics. XRFS calibration standards on Nuclepore® polycarbonate aerosol membranes expressing known (±5%) concentrations of Zn (48.4 µg/cm^2) were also imaged in parallel to the samples (Micromatter, Vancouver, BC) and used to express results as µg/cm^2. Image analysis was carried out using ImageJ (National Institutes of Health, Bethesda, MD). Regions of interest (ROI) were drawn onto the cortex (Ctx), caudate putamen (CPu), nucleus accumbens (NAc), and measurements for each ROI were obtained.

Zinc-Selenium Autometallography ($ZnSe^{AMG}$)

C57BL/6J mice were treated with 20 mg/kg cocaine daily for a total of 7 injections. 24 hours after the final injection, mice were anesthetized with a ketamine-xylazine cocktail (ket=60mg/kg + xyl=12mg/kg) and injected (i.p.) with 15 mg/kg sodium selenite (Sigma Aldrich: 214485) and placed on a heating pad while anesthetized for 60 minutes. Mice were then perfused with 0.1M phosphate buffer for 5 minutes. Brain tissue was dissected, and flash frozen in dry ice

cooled isopentane and stored at -80ºC until sectioning. Coronal brain sections (20 µm) were thaw mounted at the level of the striatum and hippocampus on positively-charged glass slides. Slides were stored at -20ºC until staining. Slides were loaded in non-metallic staining racks and allowed to reach room temperature. Slides were fixed in 95% ethanol for 15 min followed by hydration in 70% (2 min) and 50% (2 min) ethanol ending in 3 x 2 min distilled water rinses. Slides were dipped in 0.5% gelatin and air dried prior to physical development. Developer was made by mixing Gum Arabic (50% solution, 100mL), citrate buffer (2.0M, 20mL), hydroquinone (1.7g in 30mL DDH_2O), silver lactate (0.22g in 30mL H_20), and DDH_2O (200mL). Developer was poured onto slides, incubated for 60 min in the dark then quickly checked at 10 min intervals until sections are dark brown. Slides were washed in slowly flowing tap water (37ºC) for 10 min to remove gelatin then rinsed 3 x 2 min in distilled water. Slides were then incubated in 5% sodium thiosulphate (12min) and rinsed 2 x 2min in distilled water and post-fixed in 70% ethanol (30min). Optional counter stain using cresyl violet or toluidine blue (5min) followed by rinse 4 x 30 sec rinse in distilled water. Finally, slides were dehydrated in 95% ethanol (5min), 100% ethanol 2 x 5 min, xylene 2 x 5 min, and coverslipped with permount. For qualitative analysis, stained sections were imaged using brightfield microscopy. For quantitative analysis, sections were imaged using a LI-COR Odyssey (Lincoln, NE). Using ImageJ, ROIs were drawn on the Ctx, CPu and NAc. For each mouse we used 2 brain sections with 4 ROIs taken per brain region for a total of 16 sampled ROIs per region for each group. Bilateral ROIs were averaged for each region leading to a total of 8 ROIs per region per mouse.

^{65}Zn Uptake Experiments using Positron Emission Tomography (PET)

ZnT3 WT and KO mice were anesthetized with isoflurane and placed in a prone position on the scanner bed of a nanoScan PET/CT (Mediso, USA) injected intravenously (~150 µL) with $^{65}ZnCl_2$ (~2.2 MBq) and PET data were acquired for 2 hours followed by a CT scan. After scanning, animals were returned to their home cage. Scans were repeated on days 1, 3, 7, and 14. For cocaine experiments, mice were injected with $^{65}ZnCl_2$ as above and then injected immediately with saline or cocaine (20 mg/kg, i.p). Saline and cocaine injections continued daily for 7 days. Mice were scanned on Day 1 and Day 7 after $^{65}ZnCl_2$ injection as above. In all cases, the PET data were reconstructed and corrected for dead-time and radioactive decay. Qualitative and quantitative assessments of PET images were performed using the PMOD software environment (PMOD

Technologies, Zurich Switzerland). Time-activity curves were generated using manually drawn volumes of interest using the CT image as a reference. Standardized uptake values (SUV) were calculated using the formula SUV(i) = C(i) / (ID × BW) where C(i) is the activity value at a given time point (in kBq/cc), ID is the injected dose (in MBq) and BW is the animal's body weight (in kg). For voxel-wise analyses we used Statistical Parametric Mapping (SPM12, London, UK) as previously described (49). First, all the images were co-registered and masked to the reference mouse atlas in PMOD. Regional changes in uptake were assessed relative to global (whole-brain) uptake. A repeated-measures analysis of variance (ANOVA) model was used that defined saline vs. cocaine-treated mice scanned at 1- and 7-days post $^{65}ZnCl_2$ injection. Images were subtracted after intensity normalization to 100 by the proportional scaling method. After estimation of the statistical model, an contrast (Cocaine > Vehicle) was applied to reveal the effects of interest. These effects were overlaid on the reference MRI. An uncorrected *P*-value of 0.05 with a cluster threshold value of 50 were used as thresholds to determine statistical significance.

Ex vivo ^{65}Zn autoradiography

One day after the last PET scan, mice were euthanized and brain tissue was dissected, flash frozen in isopentane, and stored at -80ºC until sectioning. Tissue was sectioned and thaw mounted on positively charged glass slides. Slides were placed on BAS-IP SR 2040 E Super Resolution phosphor screens (GE Healthcare) for 14-days and imaged using a phosphor imager (Typhoon FLA 7000; GE Healthcare).

Radioligand Binding Assays

Brains from euthanized C57Bl/6J mice were removed and striata dissected and quickly frozen until use. The tissue was weighed and suspended in 10 times (w/v) of ice-cold Tris-HCl buffer (50 mM, pH 7.4). The suspension was homogenized with a Polytron homogenizer (Kinematica, Basel, Switzerland) under ice. Homogenates were centrifuged at 48,000g (50 min, 4 °C) and washed twice in the same conditions to isolate the membrane fraction. Protein was quantified by the bicinchoninic acid method (Pierce). For competition experiments, membrane suspensions (50 µg of protein/ml) were incubated in 50 mM Tris-HCl (pH 7.4) 0.5 nM of [^{3H}]WIN-35428 (Perkin-Elmer) and increasing concentrations of the indicated competing drugs (WIN-35428 or cocaine) in the presence or the absence of 100 nM, 10 µM or 1 mM of $ZnCl_2$ during 2 h

at RT. Nonspecific binding was determined in the presence of 100 µM cocaine. In all cases, free and membrane-bound radioligand were separated by rapid filtration through Whatman (Clifton, NJ) GF/B filters, pre-soaked in 0.05% polyethyleneimine by using a Brandel R48 filtering manifold (Brandel Inc., Gaithersburg, MD). The filters were washed twice with 5 ml of cold buffer and transferred to scintillation vials. Beckman Ready Safe scintillation cocktail (3.0 ml) was added, and the vials were counted the next day with a Beckman 6000 liquid scintillation counter (Beckman Coulter Instruments, Fullerton, CA) at 50% efficiency.

In vitro Autoradiography using [^{3}H]WIN-35,428

Brain tissue from WT and ZnT3 KO mice was dissected, flash frozen in isopentane, and stored at -80ºC until sectioning. Tissue was sliced on a cryostat at 16 µm and thaw mounted on positively charged glass slides and stored at -20ºC until autoradiography. Incubation Buffer consisted of 50 mM Tris-HCl (7.4 pH) and 100 mM NaCl in deionized water. [^{3}H]WIN-35,428 Total binding buffer (S.A. 82.9 Ci/mmol, Conc. 1 mCi/mL) was made in incubation buffer at a concentration of 10 nM. $ZnCl_2$ binding buffer was made using the Total binding buffer stock and adding $ZnCl_2$ for a concentration of 10 µM. Slides were pre-incubated in ice-cold incubation buffer for 20 minutes then transferred to respective radioactive incubation buffers (i.e. total or total+$ZnCl_2$) for 120 minutes on ice. Slides were then washed 2 x 1min in ice-cold 50 mM Tris-HCl (pH=7.4) then dipped (30 sec) in ice-cold deionized water. Slides were dried under stream of cool air and placed on BAS-IP TR 2025 E Tritium Screen (GE Healthcare) for 5-days and imaged using a phosphor imager (Typhoon FLA 7000; GE Healthcare). Sections were analyzed using Multigauge software (Fujifilm, Japan).

In vivo Fast Scan Cyclic Voltammetry (FSCV)

FSCV procedures follow those of recently published work from our laboratory in anesthetized mice using electrical stimulation (50). Briefly, glass sealed 100 µm carbon fiber microelectrodes were pre-calibrated with known concentrations of dopamine and changes in pH to allow for a principal component analysis (PCA) of the raw data using HDCV (UNC, Chapel Hill, NC). Dopamine was identified by cyclic voltammogram using a voltage scan from -0.3 to 1.4V at 400 V/s. During the experiment an external stimulus was applied using the tungsten electrode every 5 min comprised of 24 pulses 4ms in width at 60 Hz and 180 µA while the working

electrode was implanted in the striatum (AP: +1.5 mm; ML: ±1.0 mm; DV: -3.2 to -3.7 mm from bregma). After PCA data were analyzed to determine the DA_{Max} and DA clearance rate using a custom macro written in Igor Carbon Pro which identified peaks greater than 3x root mean square noise and fit to equation 1 where DA_{Max} represents the peak DA concentration measured, k is the rate constant, and t is time (50).

(1) $DA(t) = DA_{Max}e^{-k(t-t_0)}$

Cocaine Locomotor Sensitization

Each session during the development phase was 30 minutes and mice were only exposed to one session per day with locomotor activity quantified as distance traveled (cm). All injections were administered (i.p.). Mice were first habituated to the locomotor activity chambers (Opto-varimex ATM3, Columbus Instruments). On the next two sessions mice were injected with saline and placed in the chambers. On the following five sessions, separate groups were injected with either saline or cocaine (10 mg/kg) in a counterbalanced design. Mice were then allowed 7-days of withdrawal in the colony room and then returned to the behavior room for testing expression of sensitization. Briefly, all mice were allowed access to the activity chambers for 60 minutes followed by increasing doses of cocaine (saline, 5, 10, 20 mg/kg) every 60 minutes. Data collection was paused but chambers were not cleaned in-between cocaine dosing, each mouse was picked up, injected, and placed back in chamber to continue data collection.

Cocaine Conditioned Place Preference (CPP)

The task consisted of 10 sessions, 1 per day, in chambers with two visually distinct sides, one with clear walls and white floor and one with checkered walls and black floor. The sides were divided by a door with and without access to the other side. Locomotor activity was measured by way of time spent in each chamber as well as total distance traveled (Opto-varimex ATM3, Columbus Instruments). In the first session the mice could explore both sides of a conditioning box for 15 minutes to determine inherent side preference, designated as the Pre-Test. Using this data, the cocaine-paired side was pseudo-randomized so that mice with a preference for one side (>60%) were cocaine-paired on the other, non-preferred side. Mice with no side preference were cocaine-paired in a counterbalanced fashion. Separate groups of mice were conditioned with either a 5, 10, or 20 mg/kg dose of cocaine. In an alternating fashion for 8-days, mice were injected (i.p.)

with either saline or cocaine and placed in the predetermined drug/no drug side of the chamber for 30 minutes. The mice had no physical access to the other side but were still able to see through the clear divider wall. Each mouse had a total of 4 saline-paired days and 4 cocaine-paired days. The last session was the same as the first and designated the Test session. Time spent in the cocaine-paired chamber during the Pre-Test session (prior to conditioning) was subtracted from time spent in the cocaine-paired chamber during the Test session and expressed as the Preference score.

Mouse Intravenous Cocaine Self-Administration

Mice were implanted with jugular vein catheters under ketamine/xylazine anesthesia and using aseptic surgical techniques. A 6.0 cm length MicroRenathane (ID 0.012″, OD 0.025″; Braintree Scientific Inc., Braintree, MA, USA) catheter was inserted 1.2 cm into the right jugular vein and anchored to a 24-gauge steel cannula (Plastics One, Roanoke, VA, USA) that was bent at a 100° angle and mounted to the skull with cyanoacrylate glue and dental acrylic. A 2.5-cm extension of flexible tubing was connected to the distal end of the cannula. The mice were allowed 5–7 days for recovery, during which time 0.05 ml of a 0.9% saline solution containing 20 IU/ml heparin and 0.33 mg/ml gentamycin was infused daily through the catheter to prevent catheter clotting and infection. Thereafter, 0.05 ml of 0.9% saline solution containing 20 IU/ml heparin was infused immediately prior to and immediately following each daily self-administration session. When needed, i.v. brevital (a barbiturate) was used to test catheter patency between the self-administration sessions. During cocaine self-administration sessions, the flexible tubing extension was connected to a perfusion pump (Med Associates, Fairfax, VT) via a PE50 tubing connector. After daily self-administration sessions, the free end of the cannula guide was always kept sealed.

Operant test chambers (Med Associates, Fairfax, VT) contained two levers (active and inactive) located 2.5 cm above the floor as well as a cue light above each lever. A house light mounted on the opposite side of the chamber signaled the start of each 3 hr session and remained illuminated until the session ended. For self-administration sessions, a liquid swivel mounted on a balance arm above the chamber allowed for i.v. drug delivery in freely-moving mice. Depression of the active lever resulted in the activation of an infusion pump; depression of the inactive lever was recorded but had no scheduled consequences. Each infusion was paired with two discrete cues: illumination of the cue light above the active lever, and a cue tone that lasted for the duration of

the infusion. Experimental events were controlled by a PC programmed in Medstate Notation and connected to a Med Associates interface.

After recovery from surgery, mice (n=11 WT, n=11 KO) were placed into operant chambers and allowed to lever-press for i.v. cocaine self-administration under a fixed-ratio 1 (FR1) reinforcement schedule (i.e., each lever press leads to one cocaine infusion) for 3 h daily. Each cocaine infusion lasted 4.2 sec, during which additional active lever responses were recorded but had no consequences (i.e. non-reinforced active lever response). Mice were trained initially for a high unit dose of cocaine (1 mg/kg/infusion) to potentiate acquisition of self-administration until stable self-administration was achieved, which was defined as earning at least 20 infusions per 3 hr session and an active/inactive lever press ratio exceeding 2:1. Then the mice were switched to a multiple-dose schedule to observe the dose-dependent cocaine self-administration according to a descending cocaine dose sequence from the initial dose of 1 mg/kg/infusion (sessions 1-13) to 0.5 mg/kg/infusion (sessions 14-20), 0.25 mg/kg/infusion (sessions 21-23), 0.125 mg/kg/infusion (sessions 24-27), and 0.0625 mg/kg/infusion (sessions 28-29). Mice that did not reach stability criteria, lost catheter patency, or showed excessive high-level inactive lever responding (>100 presses per session) were excluded from further experimentation. To prevent cocaine overdose, maximally allowed cocaine infusions were 50 (0.1 and 0.5 mg/kg/infusion), 100 (0.25 mg/kg/infusion), 200 (0.125 mg/kg/infusion), or 400 (0.0625 mg/kg/infusion), respectively during each 3-h session. The number of cocaine infusions earned, and active and inactive lever responses were recorded for each session. The last 2-3 days of cocaine self-administration data at each dose were averaged and used to compare dose-response performance between WT and KO mice.

After the completion of the above cocaine dose-response experiment, the animals were switched to cocaine self-administration under PR reinforcement schedule. During PR conditions, the work requirement (lever presses) needed to receive a cocaine infusion was raised progressively within each test session according to the following PR series: 1, 2, 4, 6, 9, 12, 15, 20, 25, 32, 40, 50, 62, 77, 95, 118, 145, 178, 219, 268, 328, 402, 492, and 603 until the break point was reached. The break point was defined as the maximal workload (i.e., number of lever presses) completed for the last cocaine infusion prior to a 1-h period during which no infusions were obtained by the animal. Animals were tested for cocaine self-administration under PR reinforcement at three doses (starting at 0.25, then 1 and then 0.5 mg/kg/infusion) from days 30 to 38.

After the completion of the PR experiments, the same groups of animals continued for cocaine extinction and reinstatement tests. During extinction, syringe pumps were turned off and the cocaine-associated cue light and tone were unavailable. Thus, lever pressing was recorded but had no scheduled consequences. Extinction training continued for about 20 days until the extinction criteria were met (i.e., lever responding <20% of the self-administration baseline) for at least 3 sessions. Mice then received a 10 mg/kg i.p cocaine injection to evoke reinstatement of drug-seeking behavior. During reinstatement testing, active lever presses lead to re-exposure to the cue light and tone previously paired with cocaine infusions, but not to actual cocaine infusions. Active and inactive lever responses were recorded for each extinction and reinstatement session. Lever pressing behavior during the cocaine-primed session was compared to the average lever pressies during the last 3 days of extinction.

Custom Diets

Diets were formulated by Research Diets, Inc via use of AIN-93M mature rodent diet. The diets were compositionally identical, but one diet had an adequate amount of Zn^{2+} (30 ppm) and one diet had a deficient amount of Zn^{2+} (5 ppm). Zn^{2+} concentration in each diet was confirmed in-house via random sampling of chow pellets and TXRF (S2 Picofox, Bruker, Billerica, MA).

Body Weight and Food Intake Measurements

C56BL/6J mice arrived at the NIDA mouse colony and allowed one week of environmental acclimation with regular chow and water available *ad lib*. After acclimation period, mice were given a 30 ppm Zn^{2+} diet or a 5 ppm Zn^{2+} diet for a minimum of 35 days prior to any behavioral or physiological manipulations. Mice stayed on the diet until the completion of the experiment. Mice were individually housed and weighed 3 times per week (MWF) along with food weight to track the amount of food consumed.

Immunohistochemistry

Coronal sections were sliced on a cryostat (30 µm), collected in 6-well plates with PBS, and stored at 4ºC until use. Sections were transferred to 12-well plates and permeabilized in washing buffer (PBS + Triton X-100 0.1%) for 10 min at room temperature on shaker. Tissue was blocked in blocking buffer (BSA 3% + PBS + Triton X-100 0.1%) for 60 min at RT on shaker.

Tissue was incubated overnight in primary ZnT3 antibody (1:500) (anti-rabbit, Synaptic Systems, Goettingen, Germany) at 4ºC. Tissue was washed with washing buffer 3 x 10 min at RT then incubated in secondary antibody (Alexa 480-Rabbit 1:400, Topro (1:1200), and DAPI (1:600) for 2 hrs at RT in the dark. Tissue was washed with washing buffer 3 x 10 min, transferred to dish with PBS, mounted on positively charged glass slides, and coverslipped with aqueous mounting medium (90% glycerol + 30 mM Tris-HCl, pH 8.0) and imaged using confocal microscopy.

Statistics

Depending on experiment, we used linear regression, paired/unpaired/one sample t-tests, single/multi-factor ANOVA or a mixed effects model (to account for missing data) taking repeated measures into account when appropriate. Significant main or interaction effects were followed by posthoc comparisons with appropriate corrections. All statistical tests were evaluated at the $p \leq 0.05$ level.

Results

Striatal Zn^{2+} is low in human cocaine abusers and correlates with cocaine intake

The highest DAT density in the brain is found in the striatum (22), a region heavily implicated in cocaine addiction (23-26). We performed elemental profiling in postmortem striatal tissue derived from human cocaine abusers or matched controls (Figure 1A to C and Figure S1) using total reflection X-ray fluorescence spectroscopy (TXRF). Cocaine users had significantly lower striatal Zn^{2+} levels (Figure 1D) and these levels significantly correlated with plasma concentrations of benzoylecgonine, (Figure 1E) a stable cocaine metabolite indicative of recent cocaine use (27).

Cocaine increases synaptic Zn^{2+} levels and turnover in the striatum via ZnT3-mediated exocytosis

Unlike TXRF, synchrotron X-ray fluorescence microspectroscopy (µSXRF) allows both visualization and quantification of total Zn^{2+} in brain slices (28, 29) (Figure 2A and Figure S2). µSXRF revealed that mice exposed to daily cocaine injections (10 mg/kg, intraperitoneal (IP), 4

days) and euthanized 24 hours later had significantly greater total Zn^{2+} levels in striatal and cortical regions compared to vehicle-injected mice (Figure 2, A and B).

ZnT3 knockout (KO) mice lack the ability to package vesicular Zn^{2+} and by extension synaptic Zn^{2+} release (7). ZnT3 KO mice are healthy and do not exhibit significant behavioral or physiological abnormalities (30, 31). TXRF and μSXRF are limited in providing measures of total Zn^{2+}. Therefore, we performed Timm staining, which exclusively labels vesicular Zn^{2+} (32), in mice exposed to cocaine and ZnT3 KO mice. Vesicular Zn^{2+} was highly localized to discrete regions including cingulate cortex (Ctx), dorsomedial caudate putamen (CPu), and medial nucleus accumbens (NAc) (Figure 2C and Figure S3) (33). As expected, ZnT3 KO mice lacked vesicular Zn^{2+} (Figure 2C). Mice exposed to daily cocaine injections (20 mg/kg/day, IP, 8 days) and euthanized 24 hours later exhibited significantly lower vesicular Zn^{2+} staining compared to vehicle-treated mice (Figure 2, C and D) indicating that cocaine decreases vesicular Zn^{2+} levels.

We hypothesized that cocaine would increase synaptic Zn^{2+} levels in the striatum via ZnT3-mediated exocytosis. We exposed wildtype (WT) and ZnT3 KO mice to daily vehicle or cocaine injections (20 mg/kg/day, IP, 1 or 8 days) and euthanized them 24 hours later followed by assessment of Zn^{2+} using TXRF. Vehicle-treated ZnT3 KO mice had significantly lower Zn^{2+} than vehicle-treated WT mice in cortex (Figure S4), where ZnT3 expression and vesicular Zn^{2+} pools are high. Vehicle-treated WT and KO mice did not differ in striatal Zn^{2+}, as synaptic Zn^{2+} differences in this region under these basal circumstances were below the detection limit of TXRF (Figure 2E). However, after cocaine, WT mice had significantly greater striatal Zn^{2+} content than ZnT3 KO mice (Figure 2E) indicating that ZnT3 regulates cocaine-dependent increases in synaptic Zn^{2+}.

Brain Zn^{2+} has not been previously studied *in vivo*. ^{65}Zn produces annihilation photons at 511 keV at a low (~3%) abundance and has a physical half-life of ~244 days. We reasoned that these characteristics would be sufficient for noninvasive and longitudinal detection of Zn^{2+} uptake and kinetics using positron emission tomography (PET). To confirm, WT and ZnT3 KO mice were injected intravenously (IV) with 2 μCi/g $^{65}ZnCl_2$ and scanned using PET (Figure 2F and Figure S5). Owing to the slow kinetics and long biological and physical half-lives of Zn^{2+} (34), mice were scanned longitudinally at different days after $^{65}ZnCl_2$ injection (Figure 2F). ^{65}Zn showed rapid brain uptake, exhibited slow brain clearance and was detected up to 14 days after injection (Figure 2G and H and Figure S5). ZnT3 deletion significantly reduced brain uptake of ^{65}Zn at 7- and 14-

days post injection (Figure 2H). This was confirmed *ex vivo* using autoradiography, which further showed that ^{65}Zn brain distribution overlapped with both vesicular Zn^{2+} distribution and ZnT3 expression (Figure 2I and Figure S6). To examine effects of cocaine on ^{65}Zn brain uptake, we injected mice with $^{65}ZnCl_2$ as above followed by daily vehicle or cocaine injections (20 mg/kg/day, IP, 8 days) and performed PET. Compared to vehicle, cocaine increased uptake of ^{65}Zn in brain regions with high ZnT3 expression, including the cingulate cortex, NAc, and hippocampus but decreased it in areas of low ZnT3 expression like thalamus (Figs. 2J and Figure S7). Taken together with the aforementioned findings, this result indicates that cocaine increases synaptic Zn^{2+} turnover/metabolism.

Synaptic Zn^{2+} binds to the DAT and increases the *in vivo* potency of cocaine on DA neurotransmission

In vitro studies in cells indicate that Zn^{2+} binds to the DAT and causes i) DA reuptake inhibition and ii) increased cocaine DAT binding (17, 20, 21, 35, 36). We reproduced these findings using striatal membranes where a physiologically achievable concentration (10 µM) of Zn^{2+} (1) significantly increased cocaine affinity and binding to the DAT (Figure 3, A to C). A higher, supraphysiological concentration (1 mM), decreased cocaine affinity (Figure 3, A and B). To assess cocaine's *in vivo* effects at the DAT as a function of synaptic Zn^{2+}, we performed *in vivo* fast scan cyclic voltammetry (FSCV) in the striatum of WT and ZnT3 KO mice after electrically evoked DA release and escalating cocaine injections (5, 10, 20 mg/kg, IP) (Figure 3D to G). As expected, cocaine significantly enhanced DA release after electrical stimulation and concomitantly decreased DA clearance in WT mice (Figure 3, D, F and G). In contrast, ZnT3 KO mice exhibited significantly lower cocaine-induced DA release and faster DA clearance than WT mice (Figure 3, E to G), indicating that synaptic Zn^{2+} increases the *in vivo* potency of cocaine at the DAT by promoting DA release and delaying DA clearance.

Synaptic Zn^{2+} potentiates cocaine locomotor sensitization and reward and is required for cocaine-induced DAT upregulation and cocaine reinstatement

Based on the above findings, we hypothesized that synaptic Zn^{2+} would modulate cocaine-related behaviors. First, we tested cocaine-induced locomotor sensitization in WT and ZnT3 KO mice. WT mice showed robust development of locomotor sensitization to daily injections of

cocaine (10 mg/kg/day, IP, 5 days) (Figure 4A). KO mice sensitized to cocaine but showed significantly lower cocaine-induced locomotion than WT mice (Figure 4A). One week later, vehicle-treated and cocaine-treated mice were tested for expression of cocaine locomotor sensitization via exposure to escalating cocaine injections (5, 10, and 20 mg/kg, IP). WT mice with prior cocaine exposure (cocaine-treated) showed significantly greater locomotor activity at 5 and 10 mg/kg cocaine compared to WT mice with no prior cocaine exposure (vehicle-treated) (Figure 4B), indicating expression of locomotor sensitization. In contrast, cocaine-treated KO mice did not show a significant increase in locomotor activity compared to vehicle-treated KO mice (Figure 4C). Neither WT nor ZnT3 KO cocaine-treated mice differed from the corresponding vehicle-treated mice at 20 mg/kg (Figure 4, B and C).

Cocaine exposure upregulates DAT (25, 26, 37). To assess cocaine-induced DAT changes as a function of synaptic Zn^{2+}, mice from the above sensitization experiments were euthanized 24 hours after the last cocaine injection, the striatum was dissected, and DAT binding assays were performed using [^{3}H]WIN-35,428. Vehicle-treated WT mice did not significantly differ from vehicle- or cocaine-treated ZnT3 KO mice in [^{3}H]WIN-35,428 binding (Figure 4D). Cocaine-treated WT mice had greater [^{3}H]WIN-35,428 binding than vehicle-treated WT mice and significantly greater [^{3}H]WIN-35,428 binding than both vehicle-treated and cocaine-treated KO mice, indicating that synaptic Zn^{2+} is necessary for cocaine-induced DAT upregulation.

Next, we tested whether synaptic Zn^{2+} is involved in cocaine reward using the conditioned place preference (CPP) procedure. Using one cohort per cocaine dose, WT mice exhibited cocaine preference at 5, 10, and 20 mg/kg, whereas ZnT3 KO mice exhibited cocaine preference only at 10 and 20 mg/kg (Figure 4E).

Finally, we examined whether synaptic Zn^{2+} is involved in intravenous cocaine self-administration (SA). WT mice showed robust acquisition of cocaine SA (1 mg/kg/infusion for 13 days), as evidenced by significantly greater and sustained responding on the cocaine-reinforced active lever over the non-reinforced inactive lever on days 10 through 12 (Figure 4F). Mice were then switched to a lower cocaine dose (0.5 mg/kg/infusion for 7 days). WT mice immediately reached the maximum allowed number (50) of infusions (Figure 4G). In contrast, ZnT3 KO mice failed to acquire cocaine SA at the 1 mg/kg/infusion dose (Figure 4H). At the 0.5 mg/kg/infusion dose, ZnT3 KO mice took longer time (3 days) to learn to discriminate the cocaine-reinforced active lever over the inactive lever and took longer time (5 sessions) to reach 50 infusions (Figure

4I). After acquisition of cocaine self-administration, mice were tested at lower doses of cocaine. WT and KO mice did not differ in the number of cocaine infusions at these lower doses (Figure S8) but KO mice showed significantly lower cocaine intake at the 1 and 0.125 mg/kg/infusion doses (Figure 4J). Mice were then assessed for extinction of cocaine self-administration, but no genotype differences were observed (Figure 4K). After mice had extinguished their lever responding for cocaine, they were tested for reinstatement (relapse) responding to a cocaine priming injection (10 mg/kg, IP). WT mice showed a robust and significant reinstatement response to cocaine priming whereas KO mice did not (Figure 4L and M). In sum, these behavioral findings suggest that synaptic Zn^{2+} promotes cocaine sensitization, reward, and cocaine-seeking behavior.

Low dietary Zn^{2+} decreases brain Zn^{2+} and attenuates cocaine locomotor sensitization, reward and cocaine-induced DAT upregulation

Zn^{2+} is an essential element and chronic drug abuse (including cocaine) in humans is associated with malnutrition and dysregulated peripheral Zn^{2+} levels (8-13). Here we show that human cocaine abusers also show deficits in striatal Zn^{2+}, however, whether dietary Zn^{2+} modulates cocaine-induced behavioral effects is unknown. To examine this, we fed mice custom diets formulated with either 30 (adequate) or 5 (low) ppm Zn^{2+} (Figure 5A) for approximately one month. Diet-fed mice did not differ in body weight (Figure 5B) and the 5 ppm diet produced a decrease in food intake which lasted for only a few days after its introduction (Figure 5C). TXRF showed that mice fed the 5 ppm diet had significantly lower Zn^{2+} in cortex compared to mice fed the 30 ppm diet (Figure 5D).

Next, we performed cocaine locomotor sensitization in 30 ppm and 5 ppm mice using the same procedures as in the ZnT3 KO experiments. Both 5 ppm and 30 ppm mice developed cocaine locomotor sensitization (Figure 5E) and did not differ in cocaine-induced locomotion at this stage. However, whereas cocaine-treated 30 ppm mice showed significantly greater expression of cocaine locomotor sensitization compared to vehicle-treated 30 ppm mice (Figure 5F), cocaine-treated 5 ppm mice did not differ from vehicle-treated 5 ppm mice (Figure 5G).

30 ppm and 5 ppm mice were also assessed for cocaine preference using the same CPP procedure as in ZnT3 KO mice. 30 ppm mice showed cocaine preference at 5, 10, and 20 mg/kg, but 5 ppm mice showed cocaine preference only at 10 and 20 mg/kg (Figure 5H).

Finally, 30 ppm and 5 ppm mice exposed to escalating cocaine injections (5, 10, and 20 mg/kg, IP, one injection/hour) were euthanized 24 hours after the last injection and their brains were assessed for striatal [^{3}H]WIN-35,428 binding. 5 ppm mice exhibited significantly lower DAT binding (Figure 5J) and lower cocaine affinity (Figure 5I) compared to 30 ppm mice. In sum, these findings suggest that low dietary Zn^{2+} intake decreases brain Zn^{2+} levels, and attenuates cocaine locomotor sensitization, cocaine preference, and cocaine-induced increases in striatal DAT.

Discussion

These results are the first to describe the involvement of synaptic Zn^{2+} in regulating DA neurotransmission as well as physiological and behavioral effects to cocaine and have important implications for both general DA-dependent behaviors and especially for the prevention and treatment of cocaine addiction. Specifically, our findings suggest that dietary Zn^{2+} intake, and potentially, impaired Zn^{2+} absorption or excretion mechanisms, are implicated in cocaine reward, seeking, and relapse. As Zn^{2+} is an essential element that must be obtained from food such as oysters, meats, nuts, grains, and dairy, we propose that the Zn^{2+} deficits we identify here in human cocaine abusers arise from a combination of poor nutrition and cocaine-induced synaptic Zn^{2+} turnover/metabolism. Consequently, we suggest that the Zn^{2+} status of patients with cocaine addiction should be taken into consideration, especially since Zn^{2+} deficiency varies in prevalence across social demographics and is found in higher proportion in developing countries (38).

Our findings also expand the current understanding of cocaine neurobiology. DA and glutamate systems converge at the level of the striatum to modulate behaviors that influence cocaine seeking and abuse (24, 39). Zn^{2+}, mediated by ZnT3, is packaged with glutamate in the same synaptic vesicles and released by glutamatergic terminals in the striatum. As such, the cocaine-induced striatal Zn^{2+} changes we report likely accompany the well-described cocaine-induced increases in striatal glutamate neurotransmission (23, 24). Interestingly, Zn^{2+} binds to NMDA and AMPA receptors (40, 41) and it is likely that, in addition to DA signaling, cocaine-induced changes in synaptic Zn^{2+} may exert allosteric interactions at ionotropic glutamate receptors to influence cocaine-dependent glutamate neurotransmission and behaviors such as cocaine locomotor sensitization and cocaine priming-induced reinstatement of cocaine seeking (23, 24, 42). Finally, we propose that the cocaine-dependent changes in Zn^{2+} that we describe here

532 are not specific to cocaine but can be elicited by other psychostimulants that modulate DAT
533 function and increase corticostriatal glutamate neurotransmission (23, 24, 43), and potentially
534 other drugs of abuse, including alcohol (44)

535 Finally, in addition to its critical role in addiction, the DAT is the primary molecular target
536 for stimulant medications used in the treatment of attention-deficit hyperactivity disorder (ADHD).
537 Studies indicate that medication response is reduced in Zn^{2+}-deficient ADHD patients (45). Our
538 findings here offer a mechanistic explanation for these clinical observations and suggest that Zn^{2+}
539 supplementation may improve the efficacy of stimulant-based ADHD medications.

540 In conclusion, our findings expand current knowledge regarding the direct
541 pharmacological mechanism of action of cocaine and the brain mechanisms involved in cocaine's
542 behavioral effects by identifying a critical role for the trace element Zn^{2+} as an environmentally
543 derived modulator of cocaine affinity, potency, plasticity, reward, and seeking.

Acknowledgments and Author contributions

JLG, JB, SL, DM, KW, MLC, LAR, RJE, CJ, GB, JK, MP, MB, ZX, GT, and MM designed and/or performed experiments and/or analyzed data. ZX, GT, and MM supervised work. JLG, JB, and MM wrote the paper with input from all coauthors. The authors thank Dr. Thanos Tzounopoulos (University of Pittsburgh) for sharing ZnT3 knockout mice, Dr Richard Dyck (University of Calgary) for advice regarding Zn^{2+} staining, Dr. Yavin Shaham (NIDA) for experimental advice in behavioral experimentation and for manuscript comments, and Dr. Marisela Morales (NIDA), Dr. Antonio Lanzirotti, Dr. Keith Jones and William Rao at the National Synchrotron Light Source (NSLS) X26a Beamline at Brookhaven National Laboratory for instrumentation access. This work was supported by the NIDA Intramural Research Program (DA000069), the NIDA Medication Development Program (DA000611) and the Department of Energy (DOE) GeoSciences grant DE-FG02-92ER14244.

Conflict of Interest: The authors have declared that no conflict of interest exists.

References

1. Frederickson CJ, Suh SW, Silva D, and Thompson RB. Importance of zinc in the central nervous system: the zinc-containing neuron. *J Nutr.* 2000;130(5S Suppl):1471s-83s.
2. Gower-Winter SD, and Levenson CW. Zinc in the central nervous system: From molecules to behavior. *Biofactors.* 2012;38(3):186-93.
3. Pfeiffer CC, and Braverman ER. Zinc, the brain and behavior. *Biol Psychiatry.* 1982;17(4):513-32.
4. Sensi SL, Paoletti P, Koh JY, Aizenman E, Bush AI, and Hershfinkel M. The neurophysiology and pathology of brain zinc. *J Neurosci.* 2011;31(45):16076-85.
5. Cuajungco MP, and Lees GJ. Zinc metabolism in the brain: relevance to human neurodegenerative disorders. *Neurobiol Dis.* 1997;4(3-4):137-69.
6. Palmiter RD, Cole TB, Quaife CJ, and Findley SD. ZnT-3, a putative transporter of zinc into synaptic vesicles. *Proc Natl Acad Sci U S A.* 1996;93(25):14934-9.
7. Cole TB, Wenzel HJ, Kafer KE, Schwartzkroin PA, and Palmiter RD. Elimination of zinc from synaptic vesicles in the intact mouse brain by disruption of the ZnT3 gene. *Proc Natl Acad Sci U S A.* 1999;96(4):1716-21.
8. Santolaria-Fernandez FJ, Gomez-Sirvent JL, Gonzalez-Reimers CE, Batista-Lopez JN, Jorge-Hernandez JA, Rodriguez-Moreno F, et al. Nutritional assessment of drug addicts. *Drug Alcohol Depend.* 1995;38(1):11-8.
9. Comai S, Bertazzo A, Vachon J, Daigle M, Toupin J, Cote G, et al. Trace elements among a sample of prisoners with mental and personality disorders and aggression: correlation with impulsivity and ADHD indices. *J Trace Elem Med Biol.* 2019;51:123-9.
10. Sadlik J, Pach J, Winnik L, and Piekoszewski W. [Concentration of zinc, copper and magnesium in the serum of drug addicts]. *Przegl Lek.* 2000;57(10):563-4.
11. Cheng FL, Wang H, Wu J, Ning MX, Hu LF, and Su YL. [Determination and correlation analysis of trace elements in hair of dependence drug addicts]. *Guang Pu Xue Yu Guang Pu Fen Xi.* 2005;25(1):116-8.
12. Ruiz Martinez M, Gil Extremera B, Maldonado Martin A, Cantero-Hinojosa J, and Moreno-Abadia V. Trace elements in drug addicts. *Klin Wochenschr.* 1990;68(10):507-11.
13. Hossain KJ, Kamal MM, Ahsan M, and Islam SN. *Subst Abuse Treat Prev Policy*. 2007:12.
14. Kuhar MJ, Ritz MC, and Boja JW. The dopamine hypothesis of the reinforcing properties of cocaine. *Trends Neurosci.* 1991;14(7):299-302.
15. Volkow ND, Wang GJ, Fischman MW, Foltin RW, Fowler JS, Abumrad NN, et al. Relationship between subjective effects of cocaine and dopamine transporter occupancy. *Nature.* 1997;386(6627):827-30.
16. Wise RA, and Bozarth MA. A psychomotor stimulant theory of addiction. *Psychol Rev.* 1987;94(4):469-92.
17. Wu Q, Coffey LL, and Reith ME. Cations affect [3H]mazindol and [3H]WIN 35,428 binding to the human dopamine transporter in a similar fashion. *J Neurochem.* 1997;69(3):1106-18.
18. Scholze P, Norregaard L, Singer EA, Freissmuth M, Gether U, and Sitte HH. The role of zinc ions in reverse transport mediated by monoamine transporters. *J Biol Chem.* 2002;277(24):21505-13.

19. Liang YJ, Zhen J, Chen N, and Reith ME. Interaction of catechol and non-catechol substrates with externally or internally facing dopamine transporters. *J Neurochem.* 2009;109(4):981-94.
20. Hong WC, and Amara SG. Membrane cholesterol modulates the outward facing conformation of the dopamine transporter and alters cocaine binding. *J Biol Chem.* 2010;285(42):32616-26.
21. Norregaard L, Frederiksen D, Nielsen EO, and Gether U. Delineation of an endogenous zinc-binding site in the human dopamine transporter. *Embo j.* 1998;17(15):4266-73.
22. Ciliax BJ, Drash GW, Staley JK, Haber S, Mobley CJ, Miller GW, et al. Immunocytochemical localization of the dopamine transporter in human brain. *J Comp Neurol.* 1999;409(1):38-56.
23. Scofield MD, Heinsbroek JA, Gipson CD, Kupchik YM, Spencer S, Smith AC, et al. The Nucleus Accumbens: Mechanisms of Addiction across Drug Classes Reflect the Importance of Glutamate Homeostasis. *Pharmacol Rev.* 2016;68(3):816-71.
24. Schmidt HD, and Pierce RC. Cocaine-induced neuroadaptations in glutamate transmission: Potential therapeutic targets for craving and addiction. *Ann N Y Acad Sci.* 2010;1187:35-75.
25. Proebstl L, Kamp F, Manz K, Krause D, Adorjan K, Pogarell O, et al. Effects of stimulant drug use on the dopaminergic system: A systematic review and meta-analysis of in vivo neuroimaging studies. *Eur Psychiatry.* 2019;59:15-24.
26. Little KY, Zhang L, Desmond T, Frey KA, Dalack GW, and Cassin BJ. Striatal dopaminergic abnormalities in human cocaine users. *Am J Psychiatry.* 1999;156(2):238-45.
27. Jufer RA, Wstadik A, Walsh SL, Levine BS, and Cone EJ. Elimination of cocaine and metabolites in plasma, saliva, and urine following repeated oral administration to human volunteers. *J Anal Toxicol.* 2000;24(7):467-77.
28. Qin Z, Caruso JA, Lai B, Matusch A, and Becker JS. Trace metal imaging with high spatial resolution: applications in biomedicine. *Metallomics.* 2011;3(1):28-37.
29. Linkous DH, Flinn JM, Koh JY, Lanzirotti A, Bertsch PM, Jones BF, et al. *J Histochem Cytochem*. 2008:3-6.
30. Thackray SE, McAllister BB, and Dyck RH. Behavioral characterization of female zinc transporter 3 (ZnT3) knockout mice. *Behav Brain Res.* 2017;321:36-49.
31. Cole TB, Martyanova A, and Palmiter RD. Removing zinc from synaptic vesicles does not impair spatial learning, memory, or sensorimotor functions in the mouse. *Brain Res.* 2001;891(1-2):253-65.
32. Danscher G, and Stoltenberg M. Zinc-specific autometallographic in vivo selenium methods: tracing of zinc-enriched (ZEN) terminals, ZEN pathways, and pools of zinc ions in a multitude of other ZEN cells. *J Histochem Cytochem.* 2005;53(2):141-53.
33. Sorensen JC, Slomianka L, Christensen J, and Zimmer J. Zinc-containing telencephalic connections to the rat striatum: a combined Fluoro-Gold tracing and histochemical study. *Exp Brain Res.* 1995;105(3):370-82.
34. Takeda A, Sawashita J, and Okada S. Biological half-lives of zinc and manganese in rat brain. *Brain Res.* 1995;695(1):53-8.
35. Bjorklund NL, Volz TJ, and Schenk JO. Differential effects of Zn2+ on the kinetics and cocaine inhibition of dopamine transport by the human and rat dopamine transporters. *Eur J Pharmacol.* 2007;565(1-3):17-25.

36. Pifl C, Wolf A, Rebernik P, Reither H, and Berger ML. Zinc regulates the dopamine transporter in a membrane potential and chloride dependent manner. *Neuropharmacology.* 2009;56(2):531-40.
37. Malison RT, Best SE, van Dyck CH, McCance EF, Wallace EA, Laruelle M, et al. Elevated striatal dopamine transporters during acute cocaine abstinence as measured by [123I] beta-CIT SPECT. *Am J Psychiatry.* 1998;155(6):832-4.
38. Prasad AS. Discovery of human zinc deficiency: its impact on human health and disease. *Adv Nutr.* 2013;4(2):176-90.
39. Baker DA, McFarland K, Lake RW, Shen H, Tang XC, Toda S, et al. Neuroadaptations in cystine-glutamate exchange underlie cocaine relapse. *Nat Neurosci.* 2003;6(7):743-9.
40. Kalappa BI, Anderson CT, Goldberg JM, Lippard SJ, and Tzounopoulos T. AMPA receptor inhibition by synaptically released zinc. *Proc Natl Acad Sci U S A.* 2015;112(51):15749-54.
41. Anderson CT, Radford RJ, Zastrow ML, Zhang DY, Apfel UP, Lippard SJ, et al. Modulation of extrasynaptic NMDA receptors by synaptic and tonic zinc. *Proc Natl Acad Sci U S A.* 2015;112(20):E2705-14.
42. Fouyssac M, and Belin D. Beyond drug-induced alteration of glutamate homeostasis, astrocytes may contribute to dopamine-dependent intrastriatal functional shifts that underlie the development of drug addiction: A working hypothesis. *Eur J Neurosci.* 2019;50(6):3014-27.
43. Bonaventura J, Quiroz C, Cai NS, Rubinstein M, Tanda G, and Ferre S. Key role of the dopamine D4 receptor in the modulation of corticostriatal glutamatergic neurotransmission. *Sci Adv.* 2017;3(1):e1601631.
44. Skalny AV, Skalnaya MG, Grabeklis AR, Skalnaya AA, and Tinkov AA. Zinc deficiency as a mediator of toxic effects of alcohol abuse. *Eur J Nutr.* 2018;57(7):2313-22.
45. Lepping P, and Huber M. Role of zinc in the pathogenesis of attention-deficit hyperactivity disorder: implications for research and treatment. *CNS Drugs.* 2010;24(9):721-8.
46. Bannon MJ, Johnson MM, Michelhaugh SK, Hartley ZJ, Halter SD, David JA, et al. A molecular profile of cocaine abuse includes the differential expression of genes that regulate transcription, chromatin, and dopamine cell phenotype. *Neuropsychopharmacology.* 2014;39(9):2191-9.
47. Zhou Y, Michelhaugh SK, Schmidt CJ, Liu JS, Bannon MJ, and Lin Z. Ventral midbrain correlation between genetic variation and expression of the dopamine transporter gene in cocaine-abusing versus non-abusing subjects. *Addict Biol.* 2014;19(1):122-31.
48. Stan AD, Ghose S, Gao XM, Roberts RC, Lewis-Amezcua K, Hatanpaa KJ, et al. Human postmortem tissue: what quality markers matter? *Brain Res.* 2006;1123(1):1-11.
49. Michaelides M, Pascau J, Gispert JD, Delis F, Grandy DK, Wang GJ, et al. Dopamine D4 receptors modulate brain metabolic activity in the prefrontal cortex and cerebellum at rest and in response to methylphenidate. *Eur J Neurosci.* 2010;32(4):668-76.
50. Keighron JD, Quarterman JC, Cao J, DeMarco EM, Coggiano MA, Gleaves A, et al. Effects of (R)-Modafinil and Modafinil Analogues on Dopamine Dynamics Assessed by Voltammetry and Microdialysis in the Mouse Nucleus Accumbens Shell. *ACS Chem Neurosci.* 2019;10(4):2012-21.

Figure 1

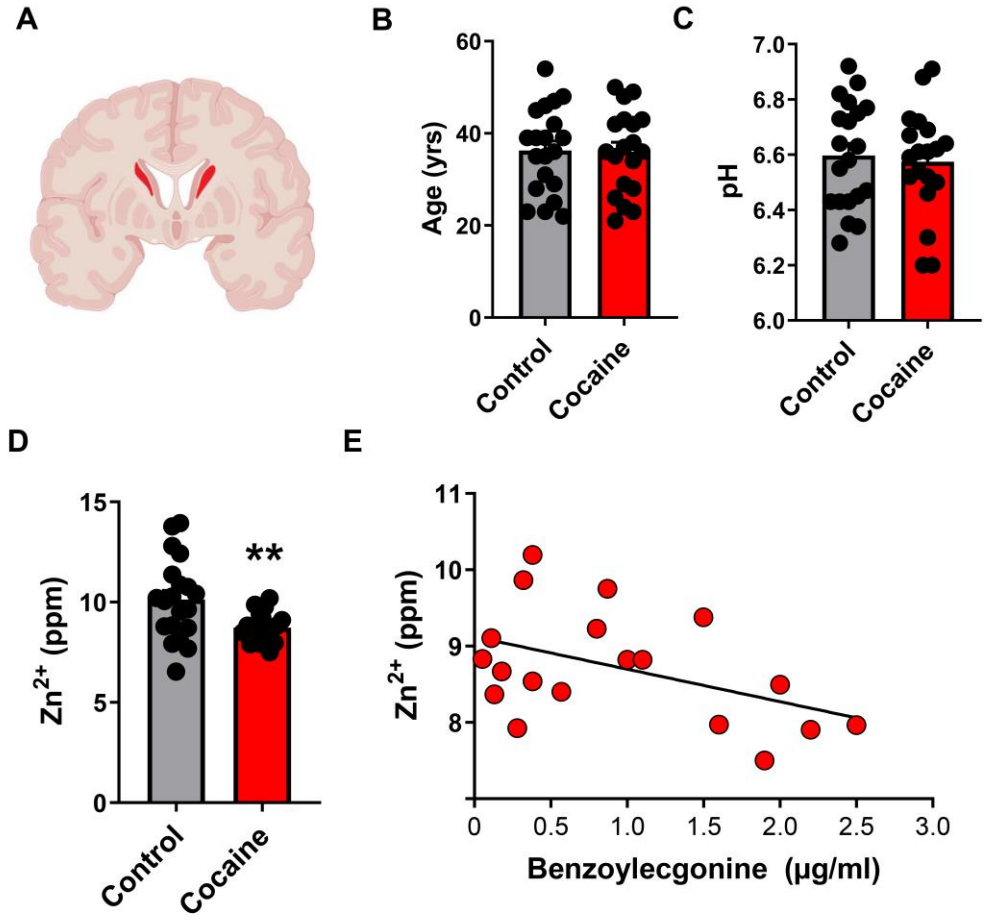

Striatal Zn^{2+} is low in human cocaine abusers and correlates with cocaine intake. (**A**) Schematic showing sampled region (caudate) from postmortem human brain. (**B**) Cocaine users (n=19) and control (n=20) subjects did not differ in age or (**C**) in tissue pH. (**D**) Cocaine users (n=19) showed significantly lower striatal Zn^{2+} (unpaired t-test, t=2.87; p=0.006) compared to control subjects (n=20). (**E**) Striatal Zn^{2+} in cocaine users (n=19) correlated significantly (linear regression; F(1, 17)=4.5; p=0.04) with plasma benzoylecgonine levels. **p≤0.05. All data expressed as Mean ±SEM.

Figure 2

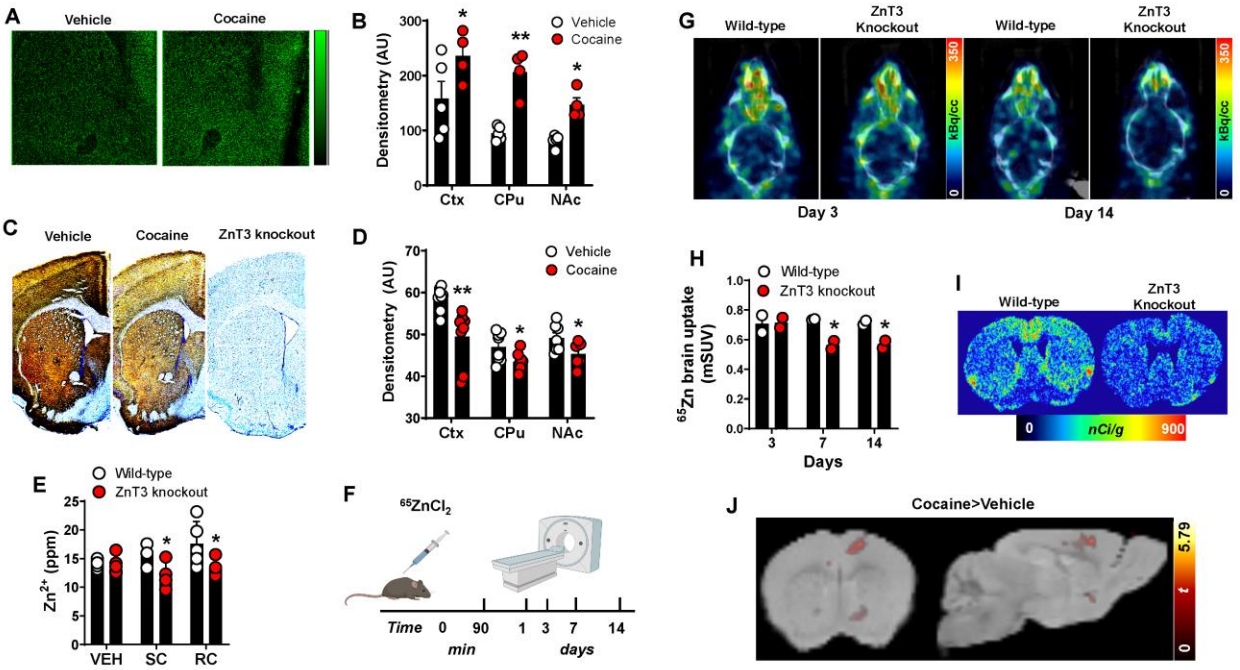

Cocaine increases synaptic Zn^{2+} levels and turnover in the striatum via ZnT3-mediated exocytosis. (**A**) Representative synchrotron X-ray fluorescence microspectroscopy (μSXRF) Zn^{2+} maps from vehicle- or cocaine-treated mice. (**B**) Cocaine-treated mice (n=4) had significantly greater (2-way anova, genotype main effect, $F(1,21)=30.11$; $p<0.001$) Zn^{2+} (AU-arbitrary units) than vehicle-treated mice (n=5) in cortex (Ctx) ($t=2.91$; $p=0.02$), caudate putamen (CPu) ($t=4.16$; $p=0.001$), and nucleus accumbens (NAc) ($t=2.44$; $p=0.02$). (**C**) Representative Timm- and cresyl violet- co-stained sections from vehicle- and cocaine-treated mice and a ZnT3 knockout mouse. (**D**) Cocaine-treated mice (n=2 mice, 8 samples/mouse/region) had significantly lower (2-way anova, genotype main effect, $F(1, 41)=24.14$; $p<0.001$) vesicular Zn^{2+} than vehicle-treated mice (n=2 mice/8 samples/mouse/region) in Ctx ($t=3.58$; $p=0.003$), CPu ($t=2.46$; $p=0.02$), and NAc ($t=2.39$; $p=0.03$). (**E**) Zn^{2+} content in wild-type and ZnT3 knockout mice exposed to vehicle (n=6 wild-type, n=9 knockout), a single cocaine injection (SC) (n=4 wild-type, n=4 knockout) or repeated cocaine injections (RC) (n=5 wild-type, n=4 knockout) injections. Wild-type mice exposed to cocaine had significantly greater (2-way anova, genotype main effect, $F(1, 26)=13.65$; $p=0.001$) Zn^{2+} levels compared to knockout mice exposed to SC ($t=2.46$; $p=0.04$) or RC injections ($t=3.07$; $p=0.01$). (**F**) PET experimental timeline. (**G**) Representative horizontal ^{65}Zn PET/CT

images from wild-type and ZnT3 knockout mice scanned at 3 and 14 days after $^{65}ZnCl_2$ administration. (**H**) ^{65}Zn brain uptake expressed as mean standard uptake value (mSUV) in wild-type (n=2) and knockout (n=2) mice scanned at 3, 7 and 14 days after injection. ZnT3 knockout mice showed significantly lower (2 way anova, genotype main effect, $F(1, 2)=34.82$, $p=0.02$) ^{65}Zn uptake at 7 ($t=3.78$; $p=0.02$) and 14 ($t=3.21$; $p=0.03$) days post injection. (**I**) Representative ^{65}Zn autoradiograms from wild-type and ZnT3 knockout mice at day 15 after $^{65}ZnCl_2$ administration. (**J**) Statistical parametric maps from vehicle- (n=4) or cocaine-treated (n=3) mice exposed to ^{65}Zn PET imaging. Cocaine-treated mice showed significantly lower ^{65}Zn uptake in Ctx and NAc (1-way anova, treatment main effect, t contrast $(1, 4)=2.13$; $p=0.049$). *$p\leq0.05$, **$p\leq0.01$. All data expressed as Mean ±SEM.

Figure 3

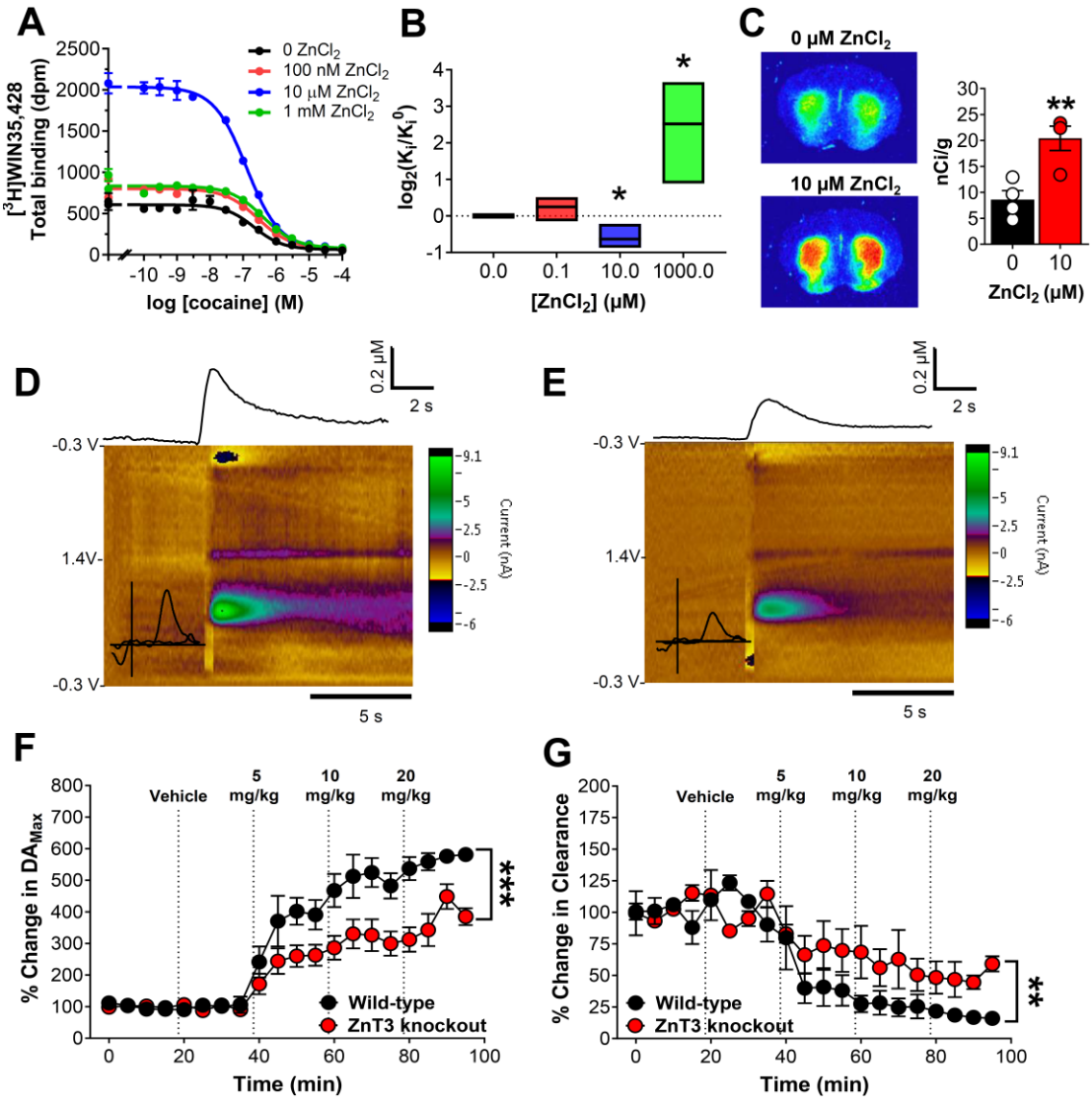

Synaptic Zn^{2+} binds to the DAT and increases the *in vivo* potency of cocaine on DA neurotransmission. (**A**) Competition binding of cocaine and $ZnCl_2$ against [^{3}H]WIN-35,428 in mouse striatal tissue (n=6 mice, combined). 10 µM $ZnCl_2$ increased and 1 mM $ZnCl_2$ decreased [^{3}H]WIN-35,428 binding (3 repetitions/curve in triplicate). (**B**) 10 µM $ZnCl_2$ significantly increased (unpaired t-test, t=3.01; p=0.03) and 1 mM $ZnCl_2$ significantly decreased (unpaired t-test, t=3.01; p=0.03) affinity of cocaine in mouse striatum (Ki (±SD) values in nM; Cocaine: 0 µM Zn, 63±39; 0.1 µM Zn, 77±57; 10 µM Zn, 43±31; 1000 µM Zn, 611±843 and WIN35,428: 0 µM Zn, 9±1.2; 0.1 µM Zn, 9.2±0.8; 10 µM Zn, 5.1±1.1; 1000 µM Zn, 13.4±1.8). (**C**) Autoradiograms

at the level of mouse striatum (n=4 mice) showing that 10 µM $ZnCl_2$ significantly increased [^{3}H]WIN-35,428 binding (unpaired t-test, t=4.03; p=0.007). (**D**) Representative fast scan cyclic voltammetry (FSCV) color plots from wild-type (n=4) and (**E**) ZnT3 knockout (n=4) mice showing dopamine (DA) responses after a 10 mg/kg IP cocaine injection. (**F**) FSCV time-course plots showing significantly lower percent change in DA_{Max} (2-way repeated measures (RM) anova; genotype x time interaction, F(19, 114)=5.46; p<0.001) and (**G**) faster DA Clearance rate (2-way RM anova; genotype x time interaction, F(19, 114)=2.35 p=0.0029) in ZnT3 knockout (n=4) compared to wild-type mice (n=4) as a function of vehicle or escalating IP cocaine injections. *p≤0.05, **p≤0.01, ***p≤0.001. All data expressed as Mean ±SEM.

Figure 4

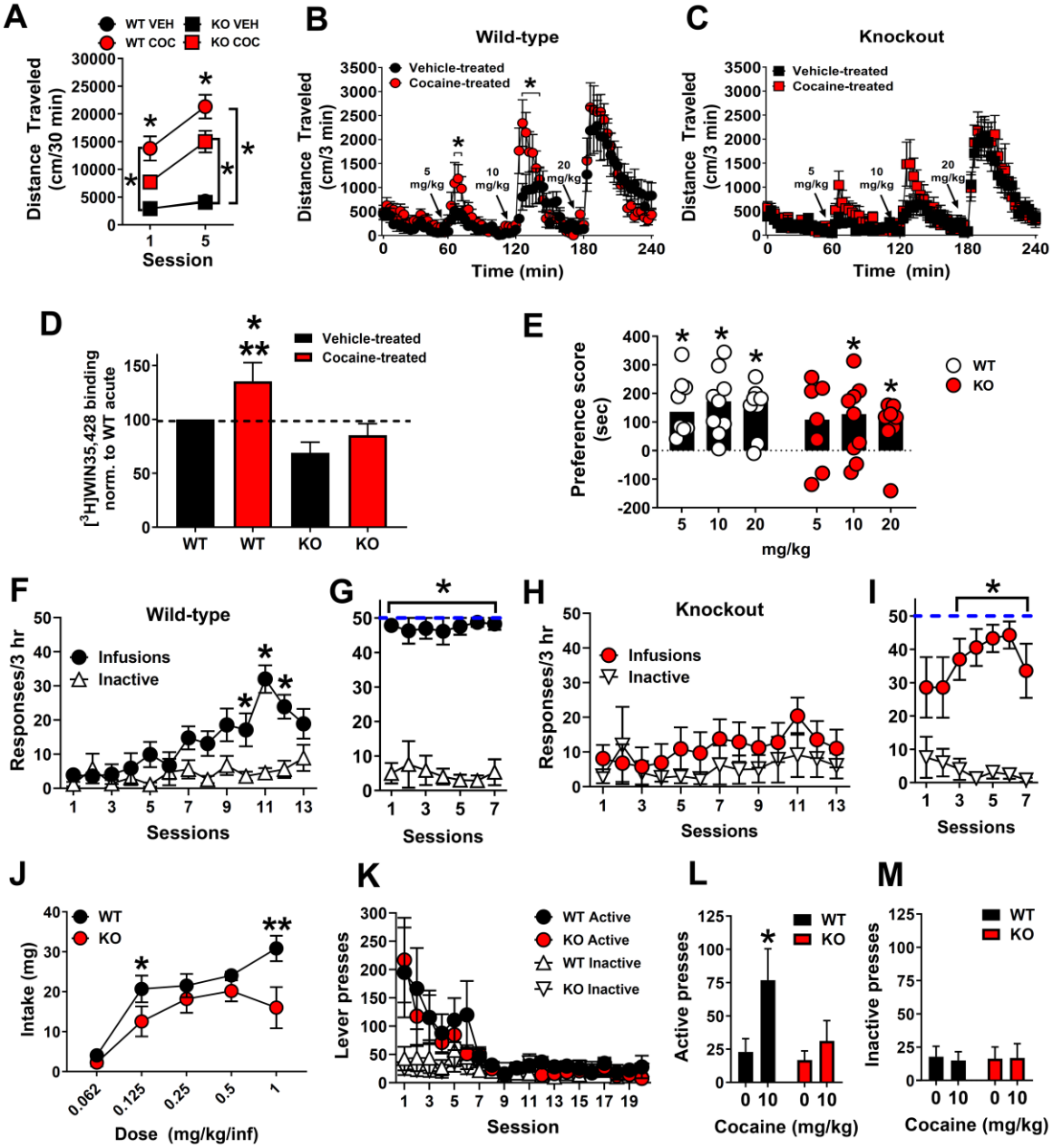

Synaptic Zn^{2+} potentiates cocaine locomotor sensitization and reward and is required for cocaine-induced DAT upregulation and cocaine reinstatement. (**A**) ZnT3 knockout (KO) mice injected daily with 10 mg/kg cocaine (COC) (n=16) showed significantly lower (2-way repeated measures (RM) anova, genotype x session interaction, $F(3, 59)=7.07$; $p=0.004$) locomotor activity on Day 1 ($t=3.09$; $p=0.01$) and Day 5 ($t=3.22$; $p=0.009$) of cocaine locomotor sensitization

compared to cocaine-injected wild-type (WT) mice (n=15). Wild-type mice injected with cocaine showed significantly greater locomotor activity than vehicle (VEH)-treated WT (n=16) mice on Day 1 ($t=5.54$; $p<0.001$) and Day 5 ($t=8.71$; $p<0.001$). KO mice injected with cocaine showed significantly greater locomotor activity than vehicle-treated KO (n=16) mice on Day 5 ($t=5.68$; $p<0.001$) but not on Day 1 ($t=2.48$; $p=0.08$). (**B**) Cocaine-treated wild-type mice (n=9) showed significantly greater (2-way RM anova, genotype x time interaction, $F(79, 1343)=1.85$; $p<0.001$) expression of cocaine locomotor sensitization at 5 (66 min; $t=3.65$; $p=0.02$, 69 min; $t=3.72$; $p=0.01$) and 10 mg/kg cocaine (123 min; $t=5.24$; $p<0.001$, 126 min; $t=6.03$; $p<0.001$, 129 min; $t=5.19$; $p<0.001$, 132 min; $t=3.75$; $p=0.01$, 135 min; $t=3.54$; $p=0.03$) compared to vehicle-treated wild-type mice (n=10). (**C**) Cocaine-treated ZnT3 knockout mice (n=10) did not show any significant difference in locomotor sensitization compared to vehicle-treated knockout mice (2-way RM anova, genotype x time interaction, $F(79, 1422)=0.9197$; $p=0.67$) (n=10). (**D**) WT mice had significantly greater DAT binding (2-way anova, genotype main effect, $F(1, 8)=12.87$; $p=0.007$) (3 repetitions per curve, in triplicate) compared to ZnT3 KO mice. Cocaine-treated WT mice (n=6) had significantly greater ($t=3.12$; $p=0.01$) DAT binding than cocaine-treated ZnT3 KO mice (n=6) and vehicle-treated KO mice (n=6) ($t=4.14$; $p=0.003$) and a trend toward significantly greater DAT binding in vehicle-treated WT mice (n=6/treatment; $t=2.19$; $p=0.059$). (**E**) WT mice showed significant preference for a chamber paired with cocaine (1 sample t-tests) at 5 (n=8, $t=4.3$; $p=0.003$), 10 (n=9, $t=4.45$; $p=0.002$), and 20 (n=8, $t=4.48$; $p=0.003$) mg/kg. ZnT3 KO mice showed significant preference for a chamber paired with cocaine at 10 (n=9, $t=2.35$; $p=0.04$) and 20 (n=7, $t=2.51$; $p=0.04$) but not at 5 mg/kg (n=7; $t=1.6$; $p=0.16$). (**F**) Wild-type mice exposed to cocaine (1 mg/kg/inf.) (n=9) showed significantly greater (mixed effects RM analysis; lever x session interaction, $F(12, 206)=3.19$; $p=0.003$) cocaine-reinforced presses compared to inactive lever presses (session 10: $t=3.07$; $p=0.02$, session 11: $t=6.21$; $p<0.001$, session 12: $t=4.15$; $p<0.001$). (**G**) Wild-type mice exposed to cocaine (0.5 mg/kg/inf.) (n=7) showed significantly greater cocaine-reinforced presses (2-way RM anova, lever main effect, $F(1, 12)=116.7$; $p<0.001$) compared to inactive lever presses (session 1: $t=12.54$; $p<0.001$, session 2: $t=5.03$; $p=0.004$, session 3: $t=7.91$; $p<0.001$, session 4: $t=9.39$; $p<0.001$, session 5: $t=15.45$; $p<0.001$, session 6: $t=23.33$; $p<0.001$, session 7: $t=10.42$; $p<0.001$). (**H**) ZnT3 knockout mice exposed to cocaine (1 mg/kg/inf.) (n=9) did not show any significant differences (2-way repeated RM anova, genotype x session interaction, $F(12, 192)=1.27$; $p=0.23$) in cocaine-reinforced or inactive lever pressing. (**I**) ZnT3 knockout mice

exposed to cocaine (0.5 mg/kg/inf.) (n=7) showed significantly greater cocaine-reinforced presses (2-way RM anova, lever x time interaction, $F(6, 71)=3.9$; $p=0.002$) compared to inactive lever presses (session 3: $t=4.74$; $p=0.007$, session 4: $t=7.03$; $p=0.002$, session 5: $t=8.86$; $p<0.001$, session 6: $t=9.82$; $p<0.001$, session 7: $t=4.01$; $p=0.04$). (**J**) ZnT3 KO mice (n=5) showed significantly lower cocaine intake (mixed effects RM analysis, genotype x dose interaction, $F(4, 44) =2.92$) at 1 mg/kg/inf. ($t=3.26$; $p=0.001$) and at 0.125 mg/kg/inf. ($t=2.03$; $p=0.04$) compared to WT mice (n=6). (**K**) WT and ZnT3 KO mice (n=5) did not differ in extinction of cocaine self-administration. (**L**) After extinction of cocaine self-administration behavior, WT mice (n=5) showed reinstatement of cocaine self-administration and significantly greater active lever presses (2-way RM anova, genotype x dose interaction, $F(1, 10)=5.09$; $p=0.04$) after cocaine priming ($t=3.17$; $p=0.005$) compared to ZnT3 KO mice (n=5). (**N**) WT (n=5) and ZnT3 KO mice (n=5) did not differ in inactive lever responding (2-way RM anova, genotype x dose interaction, $F(1, 10)=0.17$; $p=0.68$) during cocaine-primed reinstatement. *$p\leq0.05$. All data expressed as Mean ±SEM.

Figure 5

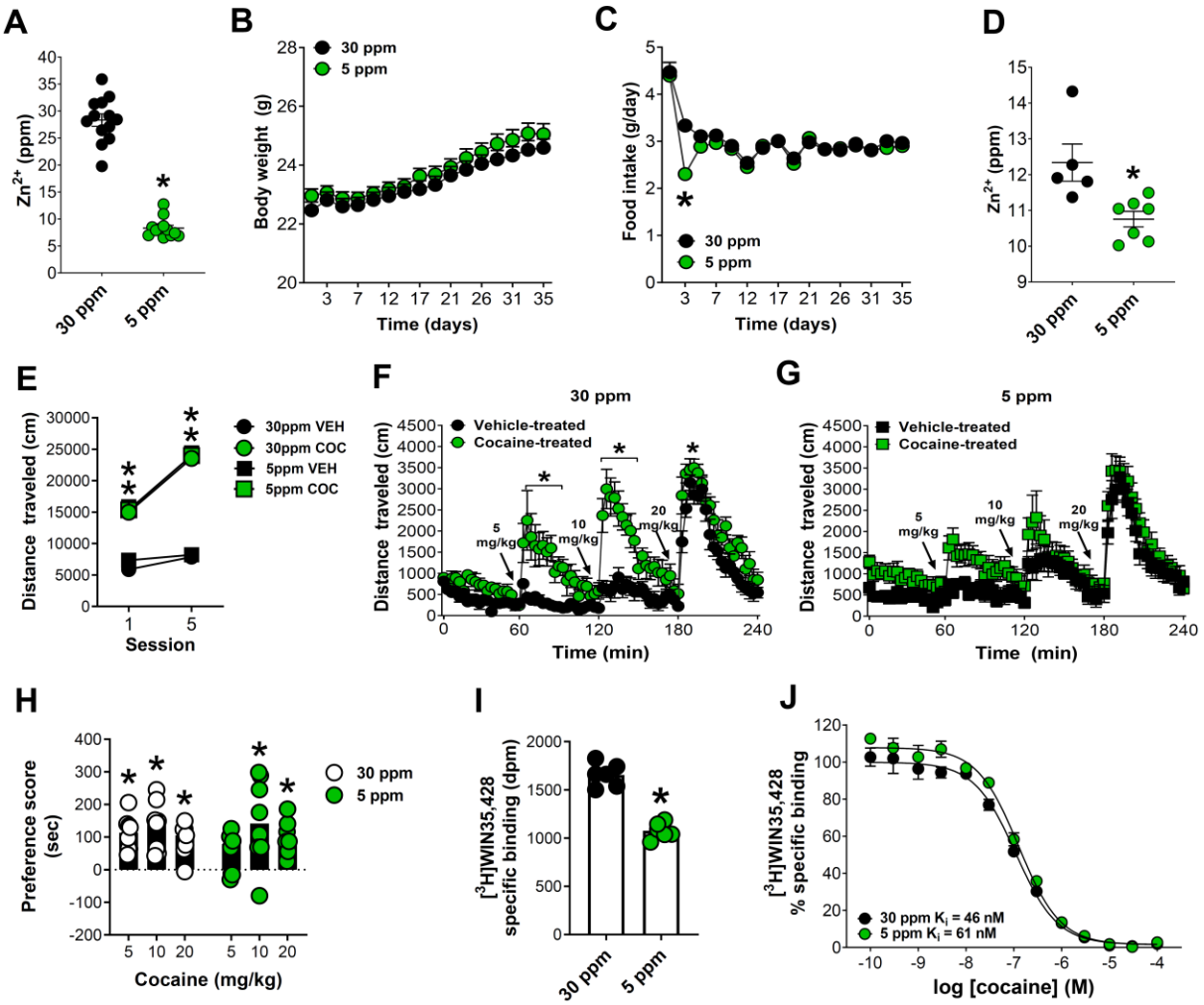

Low dietary Zn^{2+} decreases brain Zn^{2+} and attenuates cocaine locomotor sensitization, reward and cocaine-induced DAT upregulation. (**A**) Total reflection X-ray spectroscopy (TXRF)-based verification of Zn^{2+} content as a function of diet (unpaired t-test; t=15.36; p<0.001). (**B**) Mice fed a 5 ppm Zn^{2+} diet (n=32) did not differ from mice fed a 30 ppm Zn^{2+} diet (n=32) in body weight. (**C**) Mice fed a 5 ppm Zn^{2+} diet (n=32) showed a significant decrease (2-way repeated measures (RM) anova; genotype x time interaction, F(15, 930)=10.07; p<0.001) in food intake 3 days (t=11.37; p<0.001) after diet initiation compared to mice fed a 30 ppm diet (n=32). (**D**) Mice fed a 5 ppm Zn^{2+} diet (n=7) showed significantly lower total Zn^{2+} in frontal/cingulate cortex (unpaired t-test; t=3.15; p=0.01) compared to mice fed a 30 pm Zn^{2+} diet (n=5) as assessed via TXRF. (**E**) Mice fed 5 ppm or 30 ppm Zn^{2+} diets did not differ in development of cocaine (COC)

locomotor sensitization (VEH- vehicle). 30 ppm mice injected with cocaine (n=14) showed significantly greater locomotor activity (2-way RM anova; genotype x session interaction, $F(3, 52)=23.57$; $p<0.001$) than 30 ppm mice injected with vehicle (n=14) at Day 1 ($t=8.29$; $p<0.001$) and Day 5 ($t=14.27$; $p<0.001$). 5 ppm mice injected with cocaine (n=14) showed significantly greater locomotor activity compared to 5 ppm mice injected with vehicle (n=14) at Day 1 ($t=6.95$; $p<0.001$) and Day 5 ($t=13.95$; $p<0.001$). 30 ppm mice injected with cocaine showed significantly greater locomotor activity at Day 5 than on Day 1 ($t=9.98$; $p<0.001$). 5 ppm mice injected with cocaine showed significantly greater locomotor activity at Day 5 than on Day 1 ($t=10.06$; $p<0.001$). (**F**) Cocaine-treated 30 ppm diet mice (n=6) showed significantly greater expression of cocaine locomotor sensitization (2-way RM anova; genotype x time interaction, $F(79, 790)=3.98$; $p<0.001$) at 5 (66 min; $t=5.69$; $p<0.001$, 69 min; $t=4.68$; $p<0.001$, 72 min; $t=3.76$; $p=0.01$, 75 min; $t=3.78$; $p=0.01$, 78 min; $t=4.29$; $p=0.001$, 81 min; $t=3.79$; $p=0.01$, 84 min; $t=4.23$; $p=0.002$), 10 mg/kg (123 min; $t=5.37$; $p<0.001$, 126 min; $t=7.42$; $p<0.001$, 129 min; $t=6.99$; $p<0.001$, 132 min; $t=6.58$; $p=0.01$, 135 min; $t=5.08$; $p=0.03$, 138 min; $t=5.36$; $p=0.03$, 141 min; $t=4.39$; $p=0.03$, 144 min; $t=4.14$; $p=0.03$, 147 min; $t=3.78$; $p=0.03$) and 20 mg/kg cocaine (183 min; $t=3.43$; $p=0.04$) compared to vehicle-treated 30 ppm mice (n=13). (**G**) Cocaine-treated 5 ppm mice (n=6) did not show any significant difference in locomotor sensitization compared to vehicle-treated 5 ppm mice (n=6) (2-way RM anova; genotype x time interaction, $F(79, 790)=0.9342$; $p=0.64$). (**H**) Mice fed a 30 ppm Zn^{2+} diet showed significant preference (one sampled t-tests) for a chamber paired with cocaine at 5 ($t=4.3$; $p=0.003$) (n=8), 10 ($t=4.45$; $p=0.002$) (n=8), and 20 ($t=4.48$; $p=0.003$) (n=7) mg/kg. Mice fed a 5 ppm Zn^{2+} diet showed significant preference (one sample t-tests) for a chamber paired with cocaine at 10 ($t=2.35$; $p=0.04$) (n=8), and 20 ($t=2.51$; $p=0.04$) (n=8) mg/kg but not at 5 mg/kg ($t=1.6$; $p=0.16$) (n=8). (**I**) Mice exposed to cocaine and a 5 ppm Zn^{2+} diet (n=6) showed significantly lower DAT binding (unpaired t-test; $t=9.63$; $p<0.001$) (3 repetitions per group, in triplicate) and (**J**) a decrease in cocaine affinity in striatum compared to mice exposed to cocaine and a 30 ppm diet (n=6) (3 repetitions per curve, in triplicate). dpm - disintegrations per minute. *$p\leq0.05$. All data expressed as Mean ±SEM.